AIAA JOURNAL
Vol. 37, No. 4, April 1999

Characteristic-Based Treatment of Source Terms in Euler Equations for Roe Scheme

Rajendran Mohanraj,* Yedidia Neumeier,† and Ben T. Zinn‡
Georgia Institute of Technology, Atlanta, Georgia 30332-0150

The modifications required to apply Roe's Riemann solver to the Euler equations with source terms are developed and demonstrated. The generalized quasi-one-dimensional flow including the effects of friction, secondary mass addition, and energy addition has been considered. The modifications require extensions of the expressions for the strengths of the characteristic waves. The modified expressions for the wave strengths in Roe's Riemann solver are obtained from the theory of characteristics using the compatibility relations that depend on the specific source terms present. It is also shown that appropriate discretization of the source terms is required to obtain the correct solution. It is demonstrated that the compatibility relations in the presence of source terms can be used to modify not only Roe's Riemann solver but also characteristic-based boundary conditions. The validity of the proposed approach is illustrated by comparing the exact analytical solutions and the numerical solutions with and without the proposed corrections for two examples involving steady flow and one involving unsteady flow.

I. Introduction

ROE'S linearized approximate Riemann solver[1] deals with the solution of the Euler equations for an ideal gas with no source terms. In this paper, we apply Roe's solver to problems involving source terms due to mass and energy addition and to friction. We focus on the numerical solution of quasi-one-dimensional flows because they are often used to investigate the performance of complex engineering systems, e.g., combustors.[2] Examples of engineering problems whose one-dimensional representation deals with source terms include 1) mass addition at the surface of a burning solid propellant, 2) mass addition through a porous wall for cooling, and 3) flow in a supersonic wind tunnel with water vapor condensation.

The use of numerical schemes developed for homogeneous hyperbolic conservation laws in problems involving source terms without appropriately handling the source terms can produce erroneous results.[3,4] The method by which source terms are incorporated in the solution influences the stability[4,5] of the scheme. Also, the presence of source terms can alter the total variation diminishing (TVD) property[6] of the numerical scheme. More information regarding the treatment of source terms in hyperbolic problems can be obtained from Godlewski and Raviart.[7] Toro[8] discusses schemes that solve hyperbolic conservation laws with source terms by splitting the problem into advection and source term problems.

To date, Roe's Riemann solver has proven to be particularly effective in the solution of flow problems involving steep property gradients such as encountered in shock waves. Application of Roe's Riemann solver to flows involving source terms has not always been handled properly.[9] As discussed by Roe,[9] the effect of the source terms on the wave strengths needs to be considered to avoid spurious results. The manner in which this problem can be handled is illustrated by Roe[9] by considering only the effect of area change on the flow. In this paper, the effects of mass and heat additions and of friction on the compatibility relations and, thus, the wave strengths are studied.

The presence of source terms could be appropriately handled by using the projections of the source terms along the eigenvectors[4,10] as suggested by Roe.[11] An alternative approach is presented in this paper. It modifies the wave strengths by using the appropriate compatibility relations that are valid along the different characteristics in the presence of source terms. This approach is used because it is also suitable for characteristic-based treatment of the boundary conditions, which are also discussed. Finally, this approach also provides insight into the manner by which the source term modifies the physics of the problem.

The presentation starts in Sec. II with considerations of the Euler equations in the presence of source terms, a brief introduction of Roe's linearized Riemann solver, and the issues involved in accounting for the source terms. In Sec. III, Roe's approach is extended to provide a general formulation of Roe's Riemann solver for a quasi-one-dimensional flow involving area variation, mass and heat additions, and friction. Examples of the application of the developed formalism are provided in Sec. IV.

II. Source Terms and Roe's Riemann Solver for Homogeneous Euler Equations

A. Euler Equations with Source Terms

Figure 1 shows an example of a flow with secondary mass and heat additions, area variation, and friction. This flow is the subject of the paper. Within the framework of a one-dimensional analysis, the governing equations for this flow, e.g., see Refs. 12 and 13, can be rewritten in the following form:

$$(A\boldsymbol{U})_t + (A\boldsymbol{F})_x = \boldsymbol{S} \tag{1}$$

where

$$\boldsymbol{U} = \{\rho, \rho u, e\}^T \tag{2}$$

$$\boldsymbol{F} = \{\rho u, \rho u^2 + p, u(e + p)\}^T \tag{3}$$

and the total energy per unit volume e is given by

$$e = \frac{p}{(\gamma - 1)} + \frac{1}{2}\rho u^2 \tag{4}$$

for a perfect gas. The vector $\boldsymbol{S}$ describes the source terms and is given by

$$\boldsymbol{S} = \left\{ \frac{\mathrm{d}\dot{m}_s}{\mathrm{d}x}, p\frac{\mathrm{d}A}{\mathrm{d}x} - \left(\frac{\rho u|u|}{2}\right)\left(\frac{4f}{D_e}\right)A + u_{sx}\frac{\mathrm{d}\dot{m}_s}{\mathrm{d}x}, \rho u A\frac{\delta Q}{\mathrm{d}x} + H_s\frac{\mathrm{d}\dot{m}_s}{\mathrm{d}x} \right\}^T \tag{5}$$

where A is the cross-sectional area, $\mathrm{d}\dot{m}_s$ is the secondary mass addition, f is friction factor, D_e is the equivalent hydraulic diameter,

Presented as Paper 96-0766 at the AIAA 34th Aerospace Sciences Meeting, Reno, NV, Jan. 15–18, 1996; received Aug. 8, 1997; revision received Oct. 29, 1998; accepted for publication Nov. 9, 1998. Copyright © 1998 by the American Institute of Aeronautics and Astronautics, Inc. All rights reserved.

*Graduate Research Assistant, School of Aerospace Engineering. Member AIAA.
†Research Engineer, School of Aerospace Engineering. Member AIAA.
‡David S. Lewis, Jr. Chair and Regents Professor, School of Aerospace Engineering. E-mail: ben.zinn@aerospace.gatech.edu. Fellow AIAA.

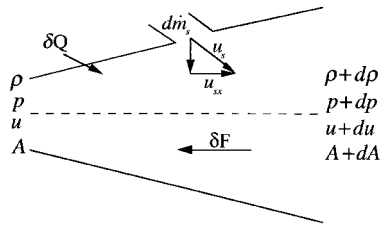

Fig. 1 Schematic of a quasi-one-dimensional flow with secondary mass addition, heat addition, area variation, and a frictional force δF.

δQ is heat addition per unit mass, u_{sx} is the x component of the secondary stream velocity, and H_s is the stagnation enthalpy per unit mass of the secondary stream. In the derivation of Eq. (1), it has been assumed that the added mass $\mathrm{d}\dot{m}_s$ and the mainstream mix completely and instantaneously to produce a stream with uniform properties at the exit of the elemental control volume. An examination of Eq. (5) shows that the expressions for the source terms do not contain derivatives of flow variables. When such derivatives are present in the source terms, they change the Jacobian matrix, i.e., see Eq. (7). In this study, the sources $\delta Q/\mathrm{d}x$ and $\mathrm{d}\dot{m}_s/\mathrm{d}x$ are specified and do not involve derivatives of flow variables.

B. Roe's Approximate Linearized Riemann Solver

This section briefly introduces the notation for Roe's Riemann solver for the one-dimensional Euler equations with no source terms to provide the background needed for modifying Roe's solver in the presence of source terms. The Euler equations for an inviscid, compressible gas flow in the absence of source terms are given by

$$\boldsymbol{U}_t + \boldsymbol{F}_x = 0 \tag{6}$$

Equation (6) can be rewritten as

$$\boldsymbol{U}_t + \boldsymbol{A}\boldsymbol{U}_x = 0 \tag{7}$$

where $\boldsymbol{A} = \partial \boldsymbol{F}/\partial \boldsymbol{U}$ is the Jacobian matrix.

Equation (7) can be solved following Roe,[1] who developed a solution for the following equation:

$$\boldsymbol{U}_t + \tilde{\boldsymbol{A}}\boldsymbol{U}_x = 0 \tag{8}$$

where $\tilde{\boldsymbol{A}}$ is a matrix constructed from the pair of states $\boldsymbol{U}_L$ and $\boldsymbol{U}_R$, which are located on the left and right sides of the interface under consideration, respectively. The requirements to be satisfied by $\tilde{\boldsymbol{A}}$ are described in Ref. 1. The most crucial of these requirements is that $\tilde{\boldsymbol{A}}$ satisfy

$$\Delta \boldsymbol{F} = \tilde{\boldsymbol{A}}\Delta \boldsymbol{U} = \tilde{\boldsymbol{A}}(\boldsymbol{U}_R - \boldsymbol{U}_L) = \sum_k \tilde{\alpha}_k \tilde{\lambda}_k \boldsymbol{e}_k \tag{9}$$

where $\tilde{\alpha}_k$, $\tilde{\lambda}_k$, and $\{\boldsymbol{e}_k\}$ are the strength of the kth wave, the kth eigenvalue of $\tilde{\boldsymbol{A}}$, and the kth right eigenvector of $\tilde{\boldsymbol{A}}$, respectively. The following expressions for these quantities are given by Roe[9]:

$$\boldsymbol{e}_1 = \{1, \tilde{u} - \tilde{a}, \tilde{H} - \tilde{u}\tilde{a}\}^T \tag{10a}$$

$$\boldsymbol{e}_2 = \{1, \tilde{u}, \tilde{u}^2/2\}^T \tag{10b}$$

$$\boldsymbol{e}_3 = \{1, \tilde{u} + \tilde{a}, \tilde{H} + \tilde{u}\tilde{a}\}^T \tag{10c}$$

$$\tilde{\lambda}_1 = \tilde{u} - \tilde{a} \tag{11a}$$

$$\tilde{\lambda}_2 = \tilde{u} \tag{11b}$$

$$\tilde{\lambda}_3 = \tilde{u} + \tilde{a} \tag{11c}$$

$$\tilde{\alpha}_1 = (1/2\tilde{a}^2)(\mathrm{d}p - \tilde{\rho}\tilde{a}\,\mathrm{d}u) \tag{12a}$$

$$\tilde{\alpha}_2 = (1/\tilde{a}^2)(\tilde{a}^2\,\mathrm{d}\rho - \mathrm{d}p) \tag{12b}$$

$$\tilde{\alpha}_3 = (1/2\tilde{a}^2)(\mathrm{d}p + \tilde{\rho}\tilde{a}\,\mathrm{d}u) \tag{12c}$$

where $H = (e + p)/\rho$ is the stagnation enthalpy per unit mass and $\mathrm{d}p$, for example, denotes $p_R - p_L$. The quantities with a tilde describe an average state obtained from $\boldsymbol{U}_L$ and $\boldsymbol{U}_R$ and are given by the following expressions:

$$\tilde{\rho} = \sqrt{\rho_L \rho_R} \tag{13}$$

$$\tilde{u} = \frac{\sqrt{\rho_L}u_L + \sqrt{\rho_R}u_R}{\sqrt{\rho_L} + \sqrt{\rho_R}} \tag{14}$$

$$\tilde{H} = \frac{\sqrt{\rho_L}H_L + \sqrt{\rho_R}H_R}{\sqrt{\rho_L} + \sqrt{\rho_R}} \tag{15}$$

$$\tilde{a}^2 = (\gamma - 1)\left[H - \frac{\tilde{u}^2}{2}\right] \tag{16}$$

C. Effect of Source Terms

To understand the physical significance of appropriately modifying the wave strengths, consider the case of heat addition (due to combustion, for example) in a one-dimensional gas flow. Following Strehlow's derivation,[14] the momentum and energy equations are

$$\rho\frac{\partial u}{\partial t} + \rho u\frac{\partial u}{\partial x} + \frac{\partial p}{\partial x} = 0 \tag{17}$$

$$\frac{\partial p}{\partial t} + \rho a^2\frac{\partial u}{\partial x} + u\frac{\partial p}{\partial x} = (\gamma - 1)\dot{q}_v \tag{18}$$

where $\dot{q}_v$ is the heat addition per unit volume per unit time. In terms of δQ,

$$\dot{q}_v = \rho u\frac{\delta Q}{\mathrm{d}x} \tag{19}$$

Multiplying Eq. (17) by the speed of sound a and adding and subtracting the resulting equation from Eq. (18) yields the following two equations:

$$\left[\frac{\partial p}{\partial t} + (u \pm a)\frac{\partial p}{\partial x}\right] \pm \rho a\left[\frac{\partial u}{\partial t} + (u \pm a)\frac{\partial u}{\partial x}\right] = (\gamma - 1)\dot{q}_v \tag{20}$$

where the equations with the + and − signs describe relationships that are valid along the right and left running Mach waves, respectively.

In the absence of heat addition, i.e., when $\dot{q}_v = 0$, the total derivative of pressure along a Mach wave, i.e., the first term in parenthesis in Eq. (20), is balanced by the product of the corresponding total derivative of velocity, i.e., the second term in parenthesis in Eq. (20), and the characteristic impedance of the medium ρa. However, the presence of heat addition changes the local relationships between the total pressure and velocity derivatives along the Mach waves. Consequently, the definitions of the strengths of the left and right running Mach waves and the entropy wave must be appropriately modified to properly incorporate the effect of heat addition.

The relationship that must be satisfied along the path line can be obtained by substituting the relationship $\rho\partial u/\partial x = -\mathrm{D}\rho/\mathrm{D}t$ (obtained from the continuity equation) into Eq. (18) to obtain

$$\frac{\mathrm{D}p}{\mathrm{D}t} - a^2\frac{\mathrm{D}\rho}{\mathrm{D}t} = (\gamma - 1)\dot{q}_v \tag{21}$$

Equation (21) shows that in the presence of a heat source changes along the pathline are not isentropic.

To develop the expressions for wave strengths in the presence of heat addition, we make use of compatibility relations. Compatibility relations describe the relationship between the total differential changes of different quantities along the characteristics for a general unsteady flow. We first demonstrate the connection between compatibility relations and wave strengths in the absence of source terms, and subsequently, we use this connection for the development of expressions for the wave strengths that account for the presence of heat addition.

In the absence of source terms, the compatibility relationship along the left running Mach wave, i.e., along the path $\mathrm{d}t = \mathrm{d}x/(u - a)$, for an unsteady flow can be obtained by choosing the negative sign in Eq. (20) and setting $\dot{q}_v$ to zero. This yields

$$\left[\frac{\partial p}{\partial t} + (u - a)\frac{\partial p}{\partial x}\right] - \rho a\left[\frac{\partial u}{\partial t} + (u - a)\frac{\partial u}{\partial x}\right] = 0 \tag{22}$$

which, after multiplying by dt, can be symbolically written as

$$dp_- - \rho a\, du_- = 0 \tag{23}$$

where dp_- and du_- are the total differential changes in pressure and velocity, respectively, along the left running Mach wave.

Though the left-hand side of Eq. (23) is of the same form as the wave strength $\tilde{\alpha}_1$ [see Eq. (12a)], the dp in Eq. (12a) denotes the change in pressure along x whereas the dp_- in Eq. (23) denotes the total differential change in pressure along the left running Mach wave. To compare Eq. (23) with Eq. (12a), we restrict our attention to steady state. At steady state, the total differential of any variable e.g., $du = (\partial u/\partial x)\,dx + (\partial u/\partial t)\,dt$, along any characteristic, i.e., for $dt = dx/(u-a)$, dx/u or $dx/(u+a)$, reduces to its variation along x. Hence, at steady state, the compatibility relation given by Eq. (23) reduces to

$$dp - \rho a\, du = 0 \tag{24}$$

Comparing Eq. (24) with Eq. (12a), we see that the wave strength $\tilde{\alpha}_1$ goes to zero at steady state. Multiplying the left-hand side of Eq. (24) by the factor $1/2a^2$ and replacing the local variables ρ and a with the Roe-averaged values $\tilde{\rho}$ and $\tilde{a}$, respectively, yields $\tilde{\alpha}_1$ [see Eq. (12a)]. Similarly, when the compatibility relations along the path line and the right running Mach wave are written in a homogeneous form, the left-hand sides yield the wave strengths $\tilde{\alpha}_2$ and $\tilde{\alpha}_3$, respectively (apart from a multiplying factor).

By extending this approach to the case where heat addition is present, one could obtain the wave strengths from the compatibility relations for a flow with heat addition. We demonstrate this derivation by repeating the derivation of the compatibility relation along the left running Mach wave including the effect of heat addition, starting from Eq. (20). Substituting Eq. (19) into Eq. (20), choosing the negative sign for the left running Mach wave, and assuming steady state, we obtain

$$(u-a)\frac{dp}{dx} - \rho a(u-a)\frac{du}{dx} = (\gamma-1)\rho u\frac{\delta Q}{dx} \tag{25a}$$

or

$$dp - \rho a\, du - \frac{(\gamma-1)\rho u \delta Q}{u-a} = 0 \tag{25b}$$

which is the compatibility relation along the left running Mach wave in the presence of heat addition, written in homogeneous form. Using this compatibility relation, the modified wave strength $\tilde{\alpha}_1$ in the presence of heat addition is chosen as

$$\tilde{\alpha}_1 = \frac{1}{2\tilde{a}^2}\left[dp - \tilde{\rho}\tilde{a}\, du - \frac{(\gamma-1)\tilde{\rho}\tilde{u}\delta Q}{\tilde{u}-\tilde{a}}\right] \tag{26}$$

to ensure that Eq. (26) reduces to Eq. (12a) when there is no heat addition.

The additional term $-(\gamma-1)\rho u\delta Q/(u-a)$ in the compatibility relationship due to the presence of heat addition [compare Eqs. (24) and (25b)] can be split into two parts that yield the effect of heat addition on dp and du separately, at steady state; that is, Eq. (25b) can be rewritten as

$$\left[dp - \frac{(\gamma-1)\rho u^2 \delta Q}{u^2-a^2}\right] - \rho a\left[du + \frac{(\gamma-1)u\delta Q}{u^2-a^2}\right] = 0 \tag{27}$$

with both the terms in parenthesis individually going to zero.

The form of Eq. (27) is directly related to the concept of influence coefficients. In compressible flow theory, the influence coefficients describe the effect of source terms on the variation of flow properties at steady state. In fact, the terms $(\gamma-1)\rho u^2\delta Q/(u^2-a^2)$ and $(\gamma-1)u\delta Q/(u^2-a^2)$ in Eq. (27) were obtained from the influence coefficients that yield the effect of the driving potential (or forcing function) dT_0/T_0 (note that $\delta Q = dH = C_p\, dT_0$ where C_p and T_0 are the specific heat at constant pressure and the stagnation temperature, respectively) on dp/p and du/u, respectively,[12,13] for a perfect gas flow. Thus, for incorporating the effect of a source term in the compatibility relations, instead of a derivation starting from the governing equations with that source term, one could use the influence coefficients for that source term. The latter approach is particularly useful in incorporating corrections due to source terms in multidimensional flows (discussed in Sec. III.B).

Once the appropriate wave strengths in the presence of source terms are known, the interface flux can be computed correctly, using the following equation[9]:

$$\boldsymbol{F}_{i+\frac{1}{2}} = \frac{1}{2}\left(\boldsymbol{F}_L + \boldsymbol{F}_R - \sum_k \tilde{\alpha}_k|\tilde{\lambda}_k|\boldsymbol{e}_k\right) \tag{28}$$

Note that at steady state, because the $\tilde{\alpha}_k$ go to zero, the numerical flux $\boldsymbol{F}_{i+\frac{1}{2}}$ equals the average of the left and right fluxes, thus representing the physical flux at the interface.

D. Source Term Discretization

The discretized form of the source term is denoted as $g_i(\boldsymbol{S})$. For example, if the scheme is explicit with first-order accuracy in time, Eq. (1) is discretized as

$$\frac{(A\boldsymbol{U})_i^{n+1} - (A\boldsymbol{U})_i^n}{\Delta t} + \frac{(A\boldsymbol{F})_{i+\frac{1}{2}}^n - (A\boldsymbol{F})_{i-\frac{1}{2}}^n}{\Delta x} = g_i(\boldsymbol{S}) \tag{29}$$

where the superscript indicates the time level. It is not appropriate to choose the function $g_i(\boldsymbol{S})$ as $\boldsymbol{S}_i$ because this can result in spurious numerical waves.[4] The function $g_i(\boldsymbol{S})$ is chosen as the weighted sum of the source vector at cell i and at neighboring cells.

Equation (29) shows that the state vector at cell i is updated using the interface fluxes at the $i+\frac{1}{2}$ and $i-\frac{1}{2}$ locations, whereas Eq. (28) shows that the interface flux depends on, other than the term

$$\sum_k \tilde{\alpha}_k|\tilde{\lambda}_k|\boldsymbol{e}_k$$

the fluxes to the left and right sides of the concerned interface with equal weight. Based on these observations, the function $g_i(\boldsymbol{S})$ is constructed in a manner that produces an algorithm in which both the source and flux vectors of a cell influence the updating of the state vector (of the same or different cells) with the same weight. This requirement is appropriate because each physical cell has a source and flux vector associated with it. This requirement is satisfied [see Eqs. (28) and (29)] by the following expression:

$$g_i(\boldsymbol{S}) = \tfrac{1}{4}\left[(\boldsymbol{S}_L)_{i-\frac{1}{2}} + (\boldsymbol{S}_R)_{i-\frac{1}{2}} + (\boldsymbol{S}_L)_{i+\frac{1}{2}} + (\boldsymbol{S}_R)_{i+\frac{1}{2}}\right] \tag{30}$$

If the scheme is first-order accurate in space, $(\boldsymbol{U}_L)_{i+\frac{1}{2}} = \boldsymbol{U}_i$ and $(\boldsymbol{U}_R)_{i+\frac{1}{2}} = \boldsymbol{U}_{i+1}$. Consequently, Eq. (30) becomes

$$g_i(\boldsymbol{S}) = \tfrac{1}{4}(\boldsymbol{S}_{i-1} + 2\boldsymbol{S}_i + \boldsymbol{S}_{i+1}) \tag{31}$$

Equation (31) may not appear as an upwind-type discretization because we make use of $\boldsymbol{S}_{i-1}$, $\boldsymbol{S}_i$, and $\boldsymbol{S}_{i+1}$ to update properties at cell i irrespective of the signs of the eigenvalues. However, we account for source terms in Roe's solver not only by choosing a particular discretization of the source term but by also modifying the wave strengths used to compute the numerical fluxes. These two modifications together constitute an upwind-based treatment of source terms. In fact, the discretization for the source term in Eq. (31) along with the appropriate modifications in the wave strengths is equivalent to a first-order scheme obtained by projecting the source terms along the eigenvectors and using upwinding,[10] as suggested by Roe.[11]

The accuracy of computing the gradient of the fluxes, i.e., $(A\boldsymbol{F})_x$, could be increased up to third order following the MUSCL approach of Van Leer,[15] where $\boldsymbol{U}_L$ and $\boldsymbol{U}_R$ are computed by the following expressions:

$$(\boldsymbol{U}_L)_{i+\frac{1}{2}} = \boldsymbol{U}_i + \tfrac{1}{4}[(1-\kappa)\nabla\boldsymbol{U}_i + (1+\kappa)\Delta\boldsymbol{U}_i] \tag{32}$$

$$(\boldsymbol{U}_R)_{i+\frac{1}{2}} = \boldsymbol{U}_{i+1} - \tfrac{1}{4}[(1-\kappa)\Delta\boldsymbol{U}_{i+1} + (1+\kappa)\nabla\boldsymbol{U}_{i+1}] \tag{33}$$

where $\nabla\boldsymbol{U}_i = \boldsymbol{U}_i - \boldsymbol{U}_{i-1}$, $\Delta\boldsymbol{U}_i = \boldsymbol{U}_{i+1} - \boldsymbol{U}_i$, and κ is a parameter that determines the spatial accuracy of the scheme. A third-order scheme is obtained when κ equals $\frac{1}{3}$. For a scheme with first-order accuracy in space, the properties are assumed to be constant within each computational cell, i.e., piecewise constant distribution.

In contrast, the MUSCL interpolation for obtaining higher-order accuracy in space involves assumption of linear or quadratic variation of properties within each cell. For simplicity, we do not consider the use of limiters, which limit the slope of variation of properties within a cell to prevent the numerical generation of oscillations around discontinuities. It is proposed to evaluate the source vector at the interface using the same interpolation that was used to obtain the state vector at the interface [see Eqs. (32) and (33)]. In other words, for a scheme with higher-order spatial accuracy, we use the same linear or quadratic approximation for variation of the source term within the computational cell as assumed for the local properties. Using the relationships given by Eqs. (32) and (33) in Eq. (30) and simplifying, we obtain

$$g_i(\boldsymbol{S}) = \tfrac{1}{4}(\boldsymbol{S}_{i-1} + 2\boldsymbol{S}_i + \boldsymbol{S}_{i+1}) + \tfrac{1}{16}(1-\kappa)(-\boldsymbol{S}_{i-2} + 2\boldsymbol{S}_i - \boldsymbol{S}_{i+2}) \tag{34}$$

For $\kappa = \frac{1}{3}$, i.e., for a third-order accurate scheme, Eq. (34) yields

$$g_i(\boldsymbol{S}) = \tfrac{1}{24}(-\boldsymbol{S}_{i-2} + 6\boldsymbol{S}_{i-1} + 14\boldsymbol{S}_i + 6\boldsymbol{S}_{i+1} - \boldsymbol{S}_{i+2}) \tag{35}$$

Other approaches for the treatment of source terms in a higher-order numerical scheme have been investigated by Ali and Kassar[5] and Glaister[16] for a scalar hyperbolic conservation law.

III. Treatment of Source Terms for Generalized Quasi-One-Dimensional Flow

A. Wave Strengths

Here we address the issue of modification of the wave strengths for a quasi-one-dimensional flow governed by Eq. (1). The correct relationships between the differential changes in the flow properties are given by the compatibility relations in the theory of characteristics. Thus, the strengths of the entropy wave and the left and right running acoustic waves could be obtained from the appropriate compatibility relations. The compatibility relations for a generalized quasi-one-dimensional flow are[12]

$$\mathrm{d}p - a^2\,\mathrm{d}\rho = \psi\,\mathrm{d}t \tag{36}$$

along the path line,

$$\mathrm{d}p - \rho a\,\mathrm{d}u = \left[-\frac{\rho u a^2}{A}\frac{\mathrm{d}A}{\mathrm{d}x} + a^2\varepsilon - a\beta + \psi\right]\mathrm{d}t \tag{37}$$

along the left running Mach wave, and

$$\mathrm{d}p + \rho a\,\mathrm{d}u = \left[-\frac{\rho u a^2}{A}\frac{\mathrm{d}A}{\mathrm{d}x} + a^2\varepsilon + a\beta + \psi\right]\mathrm{d}t \tag{38}$$

along the right running Mach wave, where

$$\varepsilon = \frac{1}{A}\frac{\mathrm{d}\dot{m}_s}{\mathrm{d}x} \tag{39}$$

$$\beta = -\left[\left(\frac{\rho u|u|}{2}\right)\left(\frac{4f}{D_e}\right) + \frac{u(1-y)}{A}\frac{\mathrm{d}\dot{m}_s}{\mathrm{d}x}\right] \tag{40}$$

$$\psi = (\gamma-1)\left[\rho u\frac{\delta Q}{\mathrm{d}x} - \mathrm{d}H_s - u\beta\right] \tag{41}$$

$$\mathrm{d}H_s = \frac{[H - H_s]}{A}\frac{\mathrm{d}\dot{m}_s}{\mathrm{d}x} \tag{42}$$

and y equals u_{sx}/u, the ratio of the x component of the secondary stream velocity to the velocity of the mainstream.

Based on the discussion in Sec. II.C, we must obtain expressions for the wave strengths that will be applicable for the flow described by Eq. (1). This is accomplished by first multiplying Eq. (36) by $-1/\tilde{a}^2$ and Eqs. (37) and (38) by $\frac{1}{2}\tilde{a}^2$. This step is needed to recover the wave strengths in the absence of source terms, i.e., see Eqs. (12a–12c). Next, the expressions for ε, β, ψ, and $\mathrm{d}H_s$ are substituted into Eqs. (36–38) and $\mathrm{d}t$ is replaced by $\mathrm{d}x/\tilde{u}$, $\mathrm{d}x/(\tilde{u}-\tilde{a})$, and $\mathrm{d}x/(\tilde{u}+\tilde{a})$ in Eqs. (36), (37), and (38), respectively. This is needed to account for the different paths along which Eqs. (36–38) are valid. Finally, the resulting equations are rewritten in a homogeneous form, whose left-hand sides are the definitions of the α_k (without the tildes). This procedure yields the following expressions for the wave strengths in the presence of the source terms given in Eq. (5):

$$\tilde{\alpha}_1 = \frac{1}{2\tilde{a}^2}\left[\mathrm{d}p - \tilde{\rho}\tilde{a}\,\mathrm{d}u + \frac{1}{(\tilde{u}-\tilde{a})}\left(\begin{array}{l}\tilde{\rho}\tilde{u}\tilde{a}^2\dfrac{\mathrm{d}A}{\tilde{A}} - [(\gamma-1)\tilde{u}+\tilde{a}]\left(\dfrac{\tilde{\rho}\tilde{u}|\tilde{u}|}{2}\right)\left(\dfrac{4f\,\mathrm{d}x}{\tilde{D}_e}\right) - (\gamma-1)\tilde{\rho}\tilde{u}\delta Q \\ -\dfrac{\mathrm{d}\dot{m}_s}{\tilde{A}}\{\tilde{u}(1-y)[(\gamma-1)\tilde{u}+\tilde{a}] + \tilde{a}^2 - (\gamma-1)(\tilde{H}-H_s)\}\end{array}\right)\right] \tag{43a}$$

$$\tilde{\alpha}_2 = \frac{1}{\tilde{a}^2}\left[\tilde{a}^2\,\mathrm{d}\rho - \mathrm{d}p + (\gamma-1)\left(\tilde{\rho}\delta Q + \left(\frac{\tilde{\rho}\tilde{u}|\tilde{u}|}{2}\right)\left(\frac{4f\,\mathrm{d}x}{\tilde{D}_e}\right) + \frac{\mathrm{d}\dot{m}_s}{\tilde{u}\tilde{A}}\left\{\tilde{u}^2(1-y) - (\tilde{H}-H_s)\right\}\right)\right] \tag{43b}$$

$$\tilde{\alpha}_3 = \frac{1}{2\tilde{a}^2}\left[\mathrm{d}p + \tilde{\rho}\tilde{a}\,\mathrm{d}u + \frac{1}{(\tilde{u}+\tilde{a})}\left(\begin{array}{l}\tilde{\rho}\tilde{u}\tilde{a}^2\dfrac{\mathrm{d}A}{\tilde{A}} - [(\gamma-1)\tilde{u}-\tilde{a}]\left(\dfrac{\tilde{\rho}\tilde{u}|\tilde{u}|}{2}\right)\left(\dfrac{4f\,\mathrm{d}x}{\tilde{D}_e}\right) - (\gamma-1)\tilde{\rho}\tilde{u}\delta Q \\ -\dfrac{\mathrm{d}\dot{m}_s}{\tilde{A}}\{\tilde{u}(1-y)[(\gamma-1)\tilde{u}-\tilde{a}] + \tilde{a}^2 - (\gamma-1)(\tilde{H}-H_s)\}\end{array}\right)\right] \tag{43c}$$

where the quantities $\tilde{A}$, f, $\tilde{D}_e$, δQ, $\mathrm{d}\dot{m}_s$, y, and H_s describe values at the interface (see the discussion in the next section).

B. Some Observations

The modifications in the wave strengths suggested by Roe[9] for the case where area variation is the only source term can be obtained from Eqs. (43a–43c) by setting all other source terms to zero. For this case, the products $\tilde{\alpha}_k\,\tilde{\lambda}_k$ are given by

$$\tilde{\alpha}_1\tilde{\lambda}_1 = \frac{\tilde{u}-\tilde{a}}{2\tilde{a}^2}(\mathrm{d}p - \tilde{\rho}\tilde{a}\,\mathrm{d}u) + \frac{\tilde{\rho}\tilde{u}}{2}\frac{\mathrm{d}A}{\tilde{A}} \tag{44a}$$

$$\tilde{\alpha}_2\,\tilde{\lambda}_2 = (\tilde{u}/\tilde{a}^2)(\tilde{a}^2\,\mathrm{d}\rho - \mathrm{d}p) \tag{44b}$$

$$\tilde{\alpha}_3\,\tilde{\lambda}_3 = \frac{\tilde{u}+\tilde{a}}{2\tilde{a}^2}(\mathrm{d}p + \tilde{\rho}\tilde{a}\,\mathrm{d}u)\frac{\tilde{\rho}\tilde{u}}{2}\frac{\mathrm{d}A}{\tilde{A}} \tag{44c}$$

and represent the fluctuations[11] in the solution due to each of the three waves. The physics of the problem requires that a sonic flow in a variable area duct is stable only when it occurs in a region where $\mathrm{d}A/\mathrm{d}x = 0$. Hence, when an eigenvalue, e.g., $\tilde{u}-\tilde{a}$ in Eq. (44a), becomes zero, then the second term in the expression for $\tilde{\alpha}_1\tilde{\lambda}_1$, i.e., $\tilde{\rho}\tilde{u}\,\mathrm{d}A/(2\tilde{A})$, also goes to zero. This ensures that there is no discontinuous switching[11] of the effect of the source term upon $(A\boldsymbol{U})_i^{n+1} - (A\boldsymbol{U})_i^n$ when an eigenvalue changes sign. Whether this is also true for other source terms (an issue raised by Roe[11]) can be determined through our approach of modifying the wave strengths by the use of appropriate compatibility relations. As an example, consider the effect of mass addition in the neighborhood of a sonic flow based on steady-state one-dimensional compressible flow theory. Mass addition causes the Mach number to increase for a subsonic flow and to decrease for a supersonic flow. No further mass addition is possible after the mainstream flow chokes at a Mach number of unity without altering the upstream conditions. Similar behavior is exhibited in the case of heat addition and friction. The singular nature of the definitions of the strengths of the waves at $\tilde{u} = \pm\tilde{a}$ reflects this feature. Thus, as discussed by Roe[9] for the case with area variation, when $\tilde{u} = \tilde{a}$ (or $-\tilde{a}$), a stable solution exists only when the coefficient of the $1/(\tilde{u}+\tilde{a})$ [or $1/(\tilde{u}-\tilde{a})$] term goes to zero [see Eqs. (43a–43c)].

Singularities exist in the definition of $\tilde{\alpha}_k$, e.g., $\tilde{\alpha}_1$ has a singularity at $\tilde{u} = \tilde{a}$ [see Eq. (43a)], but not in the product

$$\sum_k \tilde{\alpha}_k |\tilde{\lambda}_k| \boldsymbol{e}_k$$

Hence, instead of separately computing $\tilde{\alpha}_k$, $|\tilde{\lambda}_k|$, and $\boldsymbol{e}_k$, and then computing their product, analytically computed[17] expressions for

$$\sum_k \tilde{\alpha}_k |\tilde{\lambda}_k| \boldsymbol{e}_k$$

can be used to avoid dealing with singularities.

In the absence of source terms, the strengths of the waves, i.e., $\tilde{\alpha}_k$ [see Eqs. (12a–12c)], can be obtained as the elements of $T^{-1}\Delta \boldsymbol{U}$, where T is the matrix whose columns are the $\boldsymbol{e}_k$, e.g., see Ref. 18. However, in the presence of source terms, the $\tilde{\alpha}_k$ differ from the elements of $T^{-1}\Delta \boldsymbol{U}$ because $\tilde{\alpha}_k$ are dependent on the source terms, whereas the elements of $T^{-1}\Delta \boldsymbol{U}$ are not. Similarly, the expression

$$\sum_k \tilde{\alpha}_k \tilde{\lambda}_k \boldsymbol{e}_k$$

i.e., see Eq. (9), represents not just the flux difference between the two states $\boldsymbol{F}_L$ and $\boldsymbol{F}_R$, but also contains the effect of the source terms. In fact, for a flow without discontinuities (here, the Roe-averaged state approaches the physical state at the cell interface), simplification of the equation

$$\sum_k \tilde{\alpha}_k \tilde{\lambda}_k \boldsymbol{e}_k = 0$$

yields the following steady-state continuity, momentum, and energy equations:

$$\mathrm{d}(\rho u A) - \mathrm{d}\dot{m}_s = 0 \tag{45a}$$

$$\mathrm{d}p + \rho u\,\mathrm{d}u + \left(\frac{\rho u|u|}{2}\right)\left(\frac{4f\,\mathrm{d}x}{D_e}\right) + u(1-y)\frac{\mathrm{d}\dot{m}_s}{A} = 0 \tag{45b}$$

$$\rho u\,\mathrm{d}H - \rho u \delta Q + (H - H_s)\frac{\mathrm{d}\dot{m}_s}{A} = 0 \tag{45c}$$

which are equivalent to Eq. (1) in steady state and describe the effect of source terms on the steady-state variation of the flow properties. If appropriately defined, the $\tilde{\alpha}_k$ and, thus,

$$\sum_k \tilde{\alpha}_k \tilde{\lambda}_k \boldsymbol{e}_k$$

go to zero if steady state is attained and the numerical solution satisfies Eqs. (45a–45c) as expected. In this case, Eqs. (28) and (29) become

$$\frac{(A\boldsymbol{F})_{i+1} - (A\boldsymbol{F})_{i-1}}{2\Delta x} = \frac{1}{4}(\boldsymbol{S}_{i-1} + 2\boldsymbol{S}_i + \boldsymbol{S}_{i+1}) \tag{46}$$

for a first-order scheme. This represents the conservation relation at steady state for a control volume whose boundaries are the midpoints of cells $i-1$ and $i+1$.

For a flow with large gradients, the first row in

$$\sum_k \tilde{\alpha}_k \tilde{\lambda}_k \boldsymbol{e}_k = 0$$

is valid at steady state only when $\tilde{A}$ is defined as

$$\tilde{A} = \frac{\sqrt{\rho_L}A_L + \sqrt{\rho_R}A_R}{\sqrt{\rho_L} + \sqrt{\rho_R}} \tag{47}$$

In this case, the hydraulic diameter $\tilde{D}_e$ can be obtained from $\tilde{A}$. The values for δQ, y, and H_s can be chosen based on the average values for the source terms at the interface, e.g., δQ is chosen as $(\delta Q_i + \delta Q_{i+1})/2$ at the $i + \frac{1}{2}$ interface.

Roe's approximate solver was applied in the solution of the flow of real gases by Grossman and Walters,[18] Glaister,[19] and Vinokur and Montagne.[20] The forms of the wave strengths for a real gas are the same as those for a perfect gas.[18,20] The fact that a real gas is considered brings in complications only in the way the Roe-averaged state is defined, e.g., the definition of the speed of sound. Thus, one could modify the wave strengths as suggested in this work to extend Roe scheme to real gases as well.

In the work by Grossman and Cinella,[17] which applied Roe's solver to nonequilibrium flows, the enthalpy of formation is included in the total enthalpy of the gas, thus eliminating the presence of an explicit heat source term due to chemical reactions in the energy equation. The effect of the modified wave strengths has also been considered. In contrast, the formulation provided in the present study is applicable to situations where there is a need to properly account for the explicit presence of heat sources such as those produced by combustion processes (in different formulations) and radiative heat transfer. It is also applicable for energy addition by a secondary flow whose temperature does not equal that of the mainstream, e.g., transpiration cooling.

Modifications in Roe's scheme for multidimensional flows with sources can also be performed in a manner similar to the suggested modifications for the quasi-one-dimensional flow. In Sec. II.C, it was shown that the presence of source terms could be accounted for by using appropriate influence coefficients to obtain the effect of the source term on the differential changes in flow variables, e.g., see Eqs. (25b) and (27). This approach could also be applied in a multidimensional flow by using a convenient formulation[20] of the numerical flux at an interface in terms of the average flux and the differential changes in the flow variables. In addition to the mentioned modification, the issue of source term discretization should also be considered.

IV. Numerical Examples

This section provides three examples that demonstrate the need for the proposed modifications when using an explicit scheme that is first-order accurate in time and space. The suggested discretization of the source term is also studied for a third-order accurate scheme.

The first example considers a one-dimensional flow in a constant area duct with constant heat addition per unit mass along a section of the duct of length $(\frac{1}{5})\,L_d$, where L_d is the duct length. The center of the heat addition region coincides with the center of the duct. The boundary conditions require that the inlet mass and enthalpy fluxes be constant and that the pressure at the open downstream end of the duct equal the ambient pressure. The requirements at the inlet can be attained by choking the incoming flow.

The implementation of the boundary conditions is based on the method of characteristics.[21] In this, the amplitudes of the three characteristic waves L_1, L_2, and L_3 that are associated with the eigenvalues $u-a$, u, and $u+a$, respectively, are computed at the boundaries using a one-dimensional analysis. They are given by the following equations:

$$L_1 = (u-a)\left(\frac{\partial p}{\partial x} - \rho a \frac{\partial u}{\partial x}\right) \tag{48a}$$

$$L_2 = u\left(a^2\frac{\partial \rho}{\partial x} - \frac{\partial p}{\partial x}\right) \tag{48b}$$

$$L_3 = (u+a)\left(\frac{\partial p}{\partial x} + \rho a \frac{\partial u}{\partial x}\right) \tag{48c}$$

Because there is no heat addition near the boundary, computing the amplitudes of the characteristic waves does not require any modification. If heat addition exists at the boundary, the amplitudes of the characteristic waves would have to be derived by considering the effect of this source term. This issue is discussed in our second example, which accounts for the presence of friction and area variation at the boundary.

The length of the duct in the first example is 0.1 m. Solutions were obtained for 100 and 200 grid points. For the initial conditions, the pressure, temperature, and mass flux per unit area were specified as 10^5 Pa, 298 K, and 10 Kg/m^2 s, respectively, throughout the duct. In the absence of heat addition, the initial conditions describe a steady

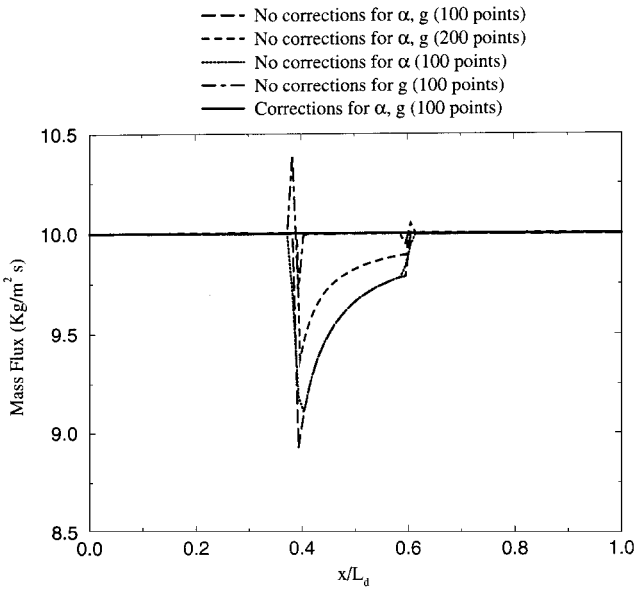

Fig. 2 Steady-state mass flux variations along the duct in the presence of a heat source, computed with and without source term corrections.

flow within the duct. At $t = 0$, the following heat addition process is introduced:

$$\delta Q = \begin{cases} 0, & 0 \le x/L_d < 0.4 \\ C_p \Delta T_0 \left(\dfrac{\mathrm{d}x}{l} \right), & 0.4 \le x/L_d < 0.6 \\ 0, & 0.6 \le x/L_d \le 1.0 \end{cases} \tag{49}$$

where $C_p = 1004.5$ J/Kg K (chosen as a constant, corresponding to the value for air), $\Delta T_0 = 1900$ K (chosen as the value for stoichiometric combustion of methane in air), and l are the specific heat at constant pressure, the increase in stagnation temperature caused due to heat addition, and the length of the region of heat addition, respectively.

To demonstrate the need to properly account for the effect of the source terms, the unsteady conservation equations were solved to determine the (final) steady flow within the duct. These solutions were obtained with and without the proposed modifications for the wave strengths and the source term discretization. The results are compared in Fig. 2. It shows that, in the absence of any corrections for the heat addition source term, the solution predicts an unrealistic "deficit" in mass flux in the heat addition region. The dependence of the error in mass flux on the grid resolution is shown in Fig. 2 by increasing the number of grid points from 100 to 200. The maximum percentage deviations from the correct steady-state mass flux are 10.7 and 6.3 for computations with 100 and 200 grid points, respectively.

If the $\tilde{\alpha}_k$ [these are used to calculate the interface flux in Eq. (28)] are computed without considering the presence of the heat addition source term, they do not go to zero when steady state is reached. This causes the physical flux to differ from the numerical flux in steady state. [The physical and numerical fluxes differ by the term

$$\left(\frac{1}{2} \right) \sum_k \tilde{\alpha}_k |\tilde{\lambda}_k| \boldsymbol{e}_k$$

that should go to zero in steady state.] In contrast, a correct solution is obtained using the approach developed in this paper [involving modifications in $\tilde{\alpha}_k$ and $g_i(\boldsymbol{S})$; see Fig. 2]. In this case, the $\tilde{\alpha}_k$ go to zero at steady state (because the $\tilde{\alpha}_k$ were appropriately defined taking heat addition into consideration), and there is no deviation between the numerical and the physical fluxes. The mass flux throughout the tube is constant at steady state as it should be.

The effects of absence of corrections in the computation of the wave strengths $\tilde{\alpha}_k$ and in the choice of the source term discretization $g_i(\boldsymbol{S})$ are also shown individually in Fig. 2. For the case involving corrections only in wave strengths but not in the source term discretization, Fig. 2 shows that errors occur in the mass flux distribution only at the boundaries of the region of heat addition. This is because the discretizations $g_i(\boldsymbol{S}) = \boldsymbol{S}_i$ and $g_i(\boldsymbol{S}) = (\boldsymbol{S}_{i-1} + 2\boldsymbol{S}_i + \boldsymbol{S}_{i+1})/4$ are equivalent if $\boldsymbol{S}_{i-1}$, $\boldsymbol{S}_i$, and $\boldsymbol{S}_{i+1}$ are equal, which, in the present example, is valid everywhere except at the boundaries of the region of heat addition.

The mass flux distribution for the case with correction only for the source term discretization but not the wave strengths is similar to that for the case with no corrections.

The expected constant distribution of mass flux at steady state is obtained when corrections are included for the wave strengths and for the source term discretization (see Fig. 2).

Because the scheme used in the preceding example is first-order accurate in space, the function $g_i(\boldsymbol{S})$ was calculated using Eq. (31). In addition, the function $g_i(\boldsymbol{S})$ in Eq. (35) was used in a scheme that is third-order accurate in space and first-order accurate in time. Although, in general, an explicit scheme involving higher-order accuracy in space and first-order accuracy in time may involve weak instability,[22,23] in the present case, convergence to the correct steady-state solution was observed. This computation with third-order accuracy in space also predicted a constant steady-state mass flux distribution along the duct in the presence of heat addition. If $g_i(\boldsymbol{S})$ is not chosen as discussed, a uniform mass flux distribution is not obtained in steady state.

The second example in this paper shows that the developed numerical approach properly accounts for the effects of source terms due to area change and friction by solving for the steady-state flow in a diverging conical duct. The diameter at the entry of the conical duct and the length of the duct are 0.01 and 0.5 m, respectively. The angle of the conical section was chosen to obtain a constant Mach number of 0.8 along the duct when the flow is steady. That is,[13]

$$\frac{\mathrm{d}M}{\mathrm{d}x} = \frac{M\{1 + [(\gamma - 1)/2]M^2\}}{1 - M^2} \left(-\frac{1}{A}\frac{\mathrm{d}A}{\mathrm{d}x} + \frac{\gamma M^2}{2}\frac{4f}{D_e} \right) = 0 \tag{50}$$

In this example, the values of f, γ, the angle of the conical section, the exit pressure, and the steady-state temperature (which is constant in space) equaled 0.05, 1.4, 1.3 deg, 10^5 Pa, and 298 K, respectively.

For initial conditions, the correct steady-state values were prescribed at the inlet and exit, and linear interpolation was used to obtain the flow variables at the intermediate points. The boundary conditions on both sides were the same as in the first example.

The L_k (where $k = 1$, 2, or 3, as for the $\tilde{\alpha}_k$) in Eqs. (48a–48c) are valid for a one-dimensional flow with no source terms. In this example, the friction and area variation source terms are non-zero at the boundaries. To be consistent in our effort to use the appropriate compatibility relations in the presence of source terms (this issue is equally applicable to the $\tilde{\alpha}_k$ and L_k), Eqs. (48a–48c) had to be modified to account for the presence of source terms.

The L_k can be obtained from the $\tilde{\alpha}_k$ because of the following similarities between them: 1) the definitions of both the $\tilde{\alpha}_k$ and L_k originate from the compatibility relations and 2) both go to zero in steady state. To see how the L_k can be obtained from the $\tilde{\alpha}_k$, it should be first noted that, because the differentials, e.g., $\mathrm{d}p$, in Eqs. (12a–12c) represent the difference between the left and the right states of an interface, dividing them by $\mathrm{d}x$ yields a partial derivative with respect to x. Multiplying Eqs. (12a–12c) (after omitting the tildes) by $2a^2(u - a)/\mathrm{d}x$, $a^2u/\mathrm{d}x$, and $2a^2(u + a)/\mathrm{d}x$ (note that $u - a$, u, and $u + a$ are the eigenvalues corresponding to L_1, L_2, and L_3), respectively, yields the expressions for L_k in Eqs. (48a–48c).

Similarly, to account for the effect of friction and area variation on the L_k, the appropriate $\tilde{\alpha}_k$ [which are obtained by neglecting terms associated with heat and mass additions in Eqs. (43a–43c)] must be used. This yields

$$L_1 = (u - a)\left(\frac{\partial p}{\partial x} - \rho a \frac{\partial u}{\partial x} \right) + \frac{\rho u a^2}{A}\frac{\mathrm{d}A}{\mathrm{d}x} - \{(\gamma - 1)u + a\}\frac{\rho u|u|}{2}\left(\frac{4f}{D_e} \right) \tag{51a}$$

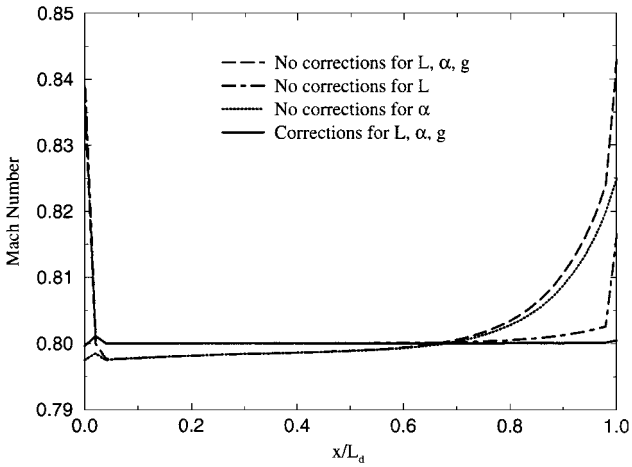

Fig. 3 Steady-state Mach number variation along the conical duct in the presence of friction calculated with and without source term corrections.

$$L_2 = u\left(a^2\frac{\partial\rho}{\partial x} - \frac{\partial p}{\partial x}\right) + (\gamma-1)u\left(\frac{\rho u|u|}{2}\right)\left(\frac{4f}{D_e}\right) \tag{51b}$$

$$L_3 = (u+a)\left(\frac{\partial p}{\partial x} + \rho a\frac{\partial u}{\partial x}\right) + \frac{\rho u a^2}{A}\frac{\mathrm{d}A}{\mathrm{d}x} - \{(\gamma-1)u - a\}\frac{\rho u|u|}{2}\left(\frac{4f}{D_e}\right) \tag{51c}$$

Note that these modifications are obtained based on the theory of characteristics, which is used in the analysis of inviscid flows. As far as the compatibility relations and their modifications are concerned, for viscous flows an inviscid approximation[21] could be used.

Solutions have been obtained with and without the proposed modifications for the $\tilde{\alpha}_k$, L_k, and $g_i(\boldsymbol{S})$. Figure 3 shows the effects of the different modifications on the steady-state Mach number distribution computed along the duct using 50 grid points. In contrast to the first example, where heat addition source term varies rapidly at the boundaries of the region of heat addition, in the present example, the source terms due to area variation and friction vary smoothly throughout the duct. Consequently, the discretizations $g_i(\boldsymbol{S}) = \boldsymbol{S}_i$ and $g_i(\boldsymbol{S}) = (\boldsymbol{S}_{i-1} + 2\boldsymbol{S}_i + \boldsymbol{S}_{i+1})/4$ yield approximately the same results, and hence the effect of source term discretization is not shown individually in Fig. 3. For cases that involve no modifications for L_k, i.e., when Eqs. (48a–48c) are used, jumps occur in the Mach number distribution at the boundaries, whereas such jumps are absent when the L_k are corrected as discussed and computed using Eqs. (51a–51c).

The Mach number distributions for the case corresponding to no corrections in α_k and for the case with no corrections in L_k, α_k and $g_i(\boldsymbol{S})$ differ mainly at the boundaries. For the latter case, the error, which is taken as the difference between the maximum and minimum values in the Mach number distribution, is 5.6% of the correct steady-state Mach number, i.e., 0.8. When all of the corrections are included, the predicted Mach number distribution is constant as expected.

Finally, we look at an example involving unsteady flow caused by mass addition.[24] Under certain conditions, it is possible to obtain an exact analytical solution for this problem. Consider a constant area duct of length L_d. The governing equations are

$$A[\boldsymbol{U}_t + \boldsymbol{F}_x] = \boldsymbol{S} \tag{52}$$

where

$$\boldsymbol{S} = \left\{\frac{\mathrm{d}\dot{m}_s}{\mathrm{d}x}, u\frac{\mathrm{d}\dot{m}_s}{\mathrm{d}x}, H\frac{\mathrm{d}\dot{m}_s}{\mathrm{d}x}\right\}^T \tag{53}$$

This corresponds to secondary mass addition along the mainstream such that the velocity and stagnation enthalpy of the secondary stream equal the corresponding local properties in the mainstream.

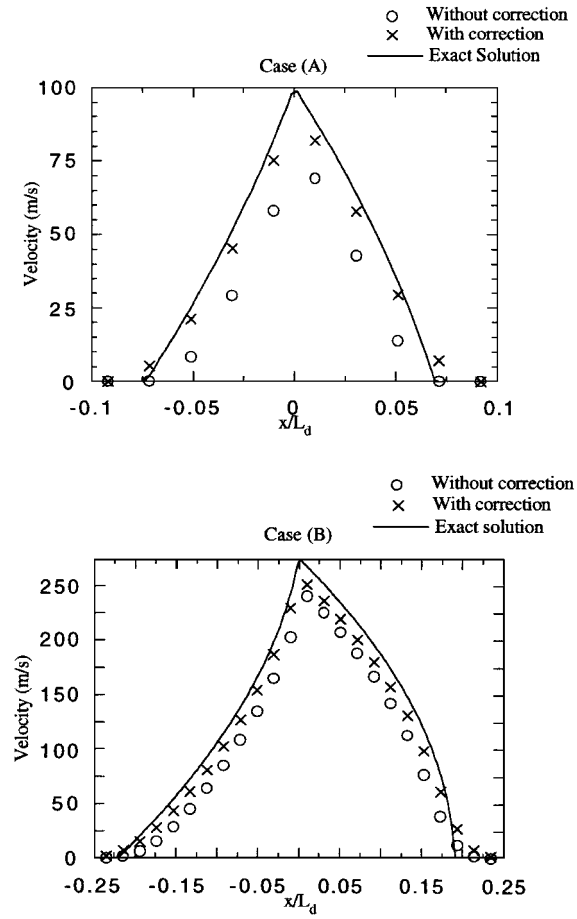

Fig. 4 Velocity variation along the duct with and without source term corrections and the exact solution for velocity at $t = 2 \times 10^{-4}$s (case A) and $t = 5.5 \times 10^{-4}$ s (case B).

To obtain the wave strengths for this case, we neglect the effect of all source terms except mass addition and substitute $y(=u_{sx}/u) = 1$, $\tilde{H} = H_s$, in Eqs. (43a–43c), which yields

$$\tilde{\alpha}_1 = \frac{1}{2\tilde{a}^2}\left[\mathrm{d}p - \tilde{\rho}\tilde{a}\,\mathrm{d}u - \frac{\tilde{a}^2\,\mathrm{d}\dot{m}_s}{(\tilde{u}-\tilde{a})\tilde{A}}\right] \tag{54a}$$

$$\tilde{\alpha}_2 = \frac{1}{\tilde{a}^2}(\tilde{a}^2\,\mathrm{d}\rho - \mathrm{d}p) \tag{54b}$$

$$\tilde{\alpha}_3 = \frac{1}{2\tilde{a}^2}\left[\mathrm{d}p + \tilde{\rho}\tilde{a}\,\mathrm{d}u - \frac{\tilde{a}^2\,\mathrm{d}\dot{m}_s}{(\tilde{u}+\tilde{a})\tilde{A}}\right] \tag{54c}$$

At $t = 0$, the fluid in the duct is at rest with uniform properties. For $t > 0$, the mass addition source term is described by

$$\frac{\mathrm{d}\dot{m}_s}{\mathrm{d}x} = \begin{cases} \rho GA/a, & -L_d/2 < x < 0 \\ 0, & 0 \le x < L_d/2 \end{cases} \tag{55}$$

where G is a constant because this choice allows us to obtain an exact analytical solution for the problem.[24] At $t = t_{\mathrm{sh}} = 4a_0/[(\gamma+1)G]$ (where a_0 is the speed of sound at $t = 0$), a shock occurs[24] in the region $x > 0$. For $t < t_{\mathrm{sh}}$, the flowfield is isentropic, and the exact solution can be analytically obtained. The properties at the boundaries are specified as constant because the chosen total time of integration is shorter than the time required for disturbances to reach the boundaries.

At $t = 0$, the pressure, temperature, and velocity are chosen as 10^5 Pa, 298 K, and 0.0 m/s throughout the duct, which is of unit length and cross-sectional area. The mass addition parameter G and the Courant–Friedrichs–Lewy number are chosen as 1×10^6 m/s^2 and 0.98, respectively, and 50 grid points are used. For our choice of a_0 and G, a shock first occurs in the flowfield at $t_{\mathrm{sh}} = 5.8 \times 10^{-4}$s.

The spatial variation of velocity obtained with and without the suggested corrections to the wave strengths and source term discretization are compared with the exact solution for the velocity[24] in Fig. 4. It shows that the corrected numerical solution is in better agreement with the exact solution.

V. Conclusions

The need to appropriately modify the strengths and amplitudes of the characteristic waves when source terms are present in the Euler equations has been demonstrated. The appropriate discretization of the source term has been presented. The developed approach of using compatibility relations from the theory of characteristics to account for source terms is not only applicable for Roe's solver but also for other issues such as characteristic-based treatment of boundary conditions.

Acknowledgments

This work was supported by Air Force Office of Scientific Research Grant F49620-93-1-0177 with M. Birkan as Grant Monitor.

References

[1]Roe, P. L., "Approximate Riemann Solvers, Parameter Vectors, and Difference Schemes," *Journal of Computational Physics*, Vol. 43, No. 2, 1981, pp. 357–372.

[2]Heiser, W. H., McClure, W. B., and Wood, C. W., "Simulating Heat Addition via Mass Addition in Variable Area Compressible Flows," *AIAA Journal*, Vol. 34, No. 5, 1996, pp. 1076–1078.

[3]Fey, M., Jeltsch, R., and Muller, S., "The Influence of a Source Term, an Example: Chemically Reacting Hypersonic Flow," *Proceedings of the Fourth International Conference on Hyperbolic Problems*, edited by A. Donato and F. Oliveri, Vieweg, Brunswick, Germany, 1992, pp. 235–245.

[4]Bermudez, A., and Vazquez, M. E., "Upwind Methods for Hyperbolic Conservation Laws with Source Terms," *Computers and Fluids*, Vol. 23, No. 8, 1994, pp. 1049–1071.

[5]Ali, F., and Kassar, M. A., "Hyperbolic Conservation Laws Having Source Terms and Donor Cell Differencing," *International Journal of Modern Physics C*, Vol. 5, No. 3, 1994, pp. 519–536.

[6]Chalabi, A., "Stable Upwind Schemes for Hyperbolic Conservation Laws with Source Terms," *IMA Journal of Numerical Analysis*, Vol. 12, No. 2, 1992, pp. 217–241.

[7]Godlewski, E., and Raviart, P. A., "Numerical Approximation of Hyperbolic Systems of Conservation Laws," *Applied Mathematical Sciences*, Vol. 118, Springer–Verlag, Berlin, 1996.

[8]Toro, E. F., *Riemann Solvers and Numerical Methods for Fluid Dynamics*, Springer–Verlag, New York, 1997, Chap. 15.

[9]Roe, P. L., "Characteristic-Based Schemes for the Euler Equations," *Annual Review of Fluid Mechanics*, Vol. 18, 1986, pp. 337–365.

[10]Glaister, P., "Flux Difference Splitting for the Euler Equations in One Spatial Coordinate with Area Variation," *International Journal for Numerical Methods in Fluids*, Vol. 8, No. 1, 1988, pp. 97–119.

[11]Roe, P. L., "Upwind Differencing for Hyperbolic Conservation Laws with Source Terms," *Proceedings of International Conference on Non-linear Hyperbolic Problems*, edited by C. Carasso, P. A. Raviart, and D. Serre, Springer–Verlag, Berlin, 1986, pp. 41–51.

[12]Zucrow, M. J., and Hoffman, J. D., *Gas Dynamics*, Wiley, New York, 1976, Vol. 1, Chap. 9, and Vol. 2, Chap. 19.

[13]Shapiro, A. H., *The Dynamics and Thermodynamics of Compressible Fluid Flow*, Vol. 1, Ronald, New York, 1953, Chap. 8.

[14]Strehlow, R. A., *Combustion Fundamentals*, McGraw–Hill, New York, 1984, Chap. 5.

[15]Van Leer, B., "Towards the Ultimate Conservative Difference Scheme. V. A Second Order Sequel to Godunov's Method," *Journal of Computational Physics*, Vol. 32, No. 1, 1979, pp. 101–136.

[16]Glaister, P., "Second Order Accurate Upwind Difference Schemes for Scalar Conservation Laws with Source Terms," *Computers and Mathematics with Applications*, Vol. 25, No. 4, 1993, pp. 65–73.

[17]Grossman, B., and Cinella, P., "The Development of Flux-Split Algorithms for Flows with Non-Equilibrium Thermodynamics and Chemical Reactions," *Proceedings of the AIAA 9th Computational Fluid Dynamics Conference*, AIAA, Washington, DC, 1988, pp. 1443–1454 (AIAA Paper 88-3595).

[18]Grossman, B., and Walters, R. W., "Analysis of Flux-Split Algorithms for Euler's Equations with Real Gases," *AIAA Journal*, Vol. 27, No. 5, 1989, pp. 524–531.

[19]Glaister, P., "An Approximate Linearised Riemann Solver for the Euler Equations for Real Gases," *Journal of Computational Physics*, Vol. 74, No. 2, 1988, pp. 382–408.

[20]Vinokur, M., and Montagne, J. L., "Generalized Flux Vector Splitting and Roe Average for an Equilibrium Real Gas," *Journal of Computational Physics*, Vol. 89, No. 2, 1990, pp. 276–300.

[21]Poinsot, T. J., and Lele, S. K., "Boundary Conditions for Direct Simulations of Compressible Viscous Flows," *Journal of Computational Physics*, Vol. 101, No. 1, 1992, pp. 104–129.

[22]Tannehill, J. C., Anderson, D. A., and Pletcher, R. H., *Computational Fluid Mechanics and Heat Transfer*, 2nd ed., Taylor and Francis, Washington, DC, 1997, p. 397.

[23]Hirsch, C., *Numerical Computation of Internal and External Flows*, Vol. 2, Wiley, New York, 1988, Chap. 21.

[24]Clarke, J. F., and Toro, E. F., "Flows Generated by Solid Propellant Burning," *Lecture Notes in Physics*, Vol. 241, Springer–Verlag, Berlin, 1985, pp. 192–205.

K. Kailasanath
Associate Editor